Modern Pathology (2020) 33:1861–1870
https://doi.org/10.1038/s41379-020-0535-y

ARTICLE

High-grade transformation of low-grade endometrial stromal sarcomas lacking *YWHAE* and *BCOR* genetic abnormalities

Youran Zou[1] · Gulisa Turashvili[2,3] · Robert A. Soslow[4] · Kay J. Park[4] · Sabrina Croce[5] · W. Glenn McCluggage[6] · Colin J. R. Stewart[7,8] · Yoshinao Oda[9] · Esther Oliva[10,11] · Robert H. Young[10,11] · Arnaud Da Cruz Paula[12] · Kimberly Dessources[12] · Charles W. Ashley[12] · Martee L. Hensley[13] · Stephen Yip[14,15,16] · Britta Weigelt[4] · Ryma Benayed[4] · Cristina R. Antonescu[4] · Cheng-Han Lee[15,16] · Sarah Chiang[4]

Received: 10 February 2020 / Revised: 19 March 2020 / Accepted: 19 March 2020 / Published online: 21 April 2020

Abstract

High-grade histologic transformation of low-grade endometrial stromal sarcoma (LGESS) is rare. Here, we describe the clinicopathologic features and gene fusion status of 12 cases (11 primary uterine corpus and 1 primary vaginal), 11 diagnosed prospectively from 2016, and 1 retrospectively collected. Targeted RNA sequencing and/or fluorescence in situ hybridization was employed in all cases. High-grade transformation was seen at the time of initial diagnosis in eight patients and at the time of recurrence in four patients, 4–11 years after initial diagnosis of LGESS. High-grade morphology consisted of generally uniform population of round to epithelioid cells with enlarged nuclei one to two times larger than a lymphocyte, visible nucleoli, and increased mitotic index (range, 6–30; median, 16 per 10 high-power fields); there was often an associated sclerotic and/or myxoid stroma. Estrogen receptor, progesterone receptor, and CD10 expression was absent or significantly decreased (compared with the low-grade component) in the high-grade foci of five tumors. One tumor demonstrated positive (diffuse and strong) cyclin D1 and BCOR staining. p53 staining was wild type in both components of all eight tumors tested. *JAZF1-SUZ12* ($n = 6$), *JAZF1-PHF1* ($n = 3$), *EPC1-PHF1*, ($n = 1$), or *BRD8-PHF1* ($n = 1$) fusions were detected in 11 tumors; no fusions were found in one by targeted RNA sequencing. Patients presented with FIGO stages I ($n = 4$), II ($n = 4$), III ($n = 1$), and IV disease ($n = 2$). Median overall survival calculated from the time of histologic transformation was 22 months (range, 8 months to 8 years) with five patients who died of disease 8–18 months after transformation. High-grade transformation may occur in LGESS with *JAZF1* and *PHF1* rearrangements at the time of or years after initial diagnosis. Such high-grade transformation is characterized by nuclear enlargement, prominent nucleoli, and increased mitotic index compared with typical LGESS. Histologic high-grade transformation may herald aggressive behavior.

Introduction

The classification of high-grade endometrial stromal sarcomas (HGESS) has significantly evolved in recent years due to the improved recognition of their distinctive morphologic, immunohistochemical, and molecular genetic aberrations. Endometrial stromal sarcoma was initially divided into low-grade and high-grade forms based on mitotic activity [1]. But the use of the term HGESS was discouraged after mitotic index was not shown to predict recurrence in stage I tumors [2]. Recent studies identified endometrial stromal sarcomas harboring *YWHAE-NUTM2* gene fusion [3–6], *ZC3H7B-BCOR* gene fusion [7, 8], and *BCOR* internal tandem duplication [9–11]. Collectively, these sarcoma types are considered histologically high-grade due to increased cytologic atypia and mitotic activity unacceptable for low-grade endometrial stromal sarcoma (LGESS). HGESS likely also encompasses lesions that demonstrate similar morphology and harbor other genetic events that have yet to be characterized [6]. A trend toward

Co-principal investigators: Cheng-Han Lee, Sarah Chiang

✉ Cheng-Han Lee
chiangs@mskcc.org

✉ Sarah Chiang
chenghan.lee@bccancer.bc.ca

Extended author information available on the last page of the article

more aggressive clinical behavior and increased frequency of lymph node metastasis compared with LGESS has been reported in HGESS [4, 6, 7, 11]. This has resulted in HGESS being reborn, but as entities with distinctive and unique molecular alterations.

There is considerable morphologic and immunohistochemical overlap among HGESS with *YWHAE* fusion and *BCOR* genetic abnormalities. *YWHAE-NUTM2* fusion-positive tumors consist of high-grade round cells arranged in sheets and/or nests that are often associated with a low-grade spindle cell component resembling fibromyxoid LGESS [3, 4, 6]. *ZC3H7B-BCOR* fusion-positive tumors consist of high-grade spindle cells, often associated with a myxoid matrix [7, 8]. Lesions harboring *BCOR* internal tandem duplication demonstrate features of both *YWHAE-NUTM2* and *ZC3H7B-BCOR* fusion-positive tumors and exhibit both spindle and round cell features [9–11]. The high-grade round cell component of HGESS harboring *YWHAE-NUTM2* fusion is characterized by diffuse and strong cyclin D1 and BCOR staining and absent CD10, estrogen receptor (ER), and progesterone receptor (PR) expression [6, 9, 12]. CD10 and cyclin D1 staining with variable ER, PR, and BCOR expression is seen in *ZC3H7B-BCOR* fusion-positive tumors [7, 9]. Endometrial stromal sarcomas with *BCOR* internal tandem duplication demonstrate strong and diffuse cyclin D1 and BCOR staining with variable CD10 expression [9–11].

Rare examples of endometrial stromal sarcoma with both low-grade and high-grade features or tumors initially diagnosed as LGESS followed later by metastatic HGESS have been reported [6, 13–16]. These lesions have been referred to as mixed low- and high-grade endometrial stromal sarcoma [15], transition of low- to high-grade [14] and de-differentiated endometrial stromal sarcoma [17]. However, all published studies of these rare lesions lack genotypic data. In this study, we aim to describe the clinicopathologic and genetic features of a series of such cases and discuss the classification of this subset of endometrial stromal tumors.

Materials and methods

Case selection

From 2016 to 2018, 11 endometrial stromal sarcoma with both low-grade and high-grade morphologic features and lacking *YWHAE* and *BCOR* genetic abnormalities were prospectively identified from the Pathology Service at Memorial Sloan Kettering Cancer Center, New York, NY, USA ($n = 5$); BC Cancer Agency, Vancouver, British Columbia, Canada ($n = 2$); King Edward Memorial Hospital, Perth, Western Australia, Australia ($n = 1$); and the consultation files of three authors (EO, RHY, WGM) at Massachusetts General Hospital, Boston, MA, USA ($n = 2$), and Belfast Health and Social Care Trust, Belfast, Northern Ireland, UK ($n = 1$). An additional case diagnosed in 2008 and originating from Kyushu University, Higashi-ku, Fukuoka, Japan was retrospectively reviewed and included in the study. Hematoxylin and eosin and immunohistochemical stained slides were reviewed. The site of histologic high-grade transformation was documented as primary (within the primary uterine or vaginal neoplasm) or metastatic (outside the uterus or vagina). Metastatic disease was further classified as synchronous, defined as the diagnosis of metastasis at the same time or within a 3-month interval of the primary tumor, or metachronous, defined as being identified after an interval of three months. Clinical data, including demographics, presentation, treatment, and follow-up, were obtained. Time to transformation was defined as the date of initial LGESS diagnosis to date of high-grade transformation. Overall survival from date of histologic diagnosis of transformation was defined as the date of transformation to date of death. Patients who did not die of disease were right censored at last follow-up.

Immunohistochemistry

CD10, ER, PR, cyclin D1, BCOR, and p53 immunohistochemical stains were performed either at the referring hospitals when reporting the cases or during the preparation of this report [7, 9, 18]; not all of the markers were performed in every case due to lack of available material. BCOR and cyclin D1 staining were interpreted as positive if ≥50% of tumor cells showed nuclear staining and negative if nuclear staining was present in <50% of cells, as previously described [12, 19]. ER and PR staining were interpreted as positive if ≥1% of tumor cells showed nuclear staining and negative if nuclear staining in <1% of cells was observed, as previously described [20]. Intensity and percentage of cells with ER and PR staining were also recorded. p53 staining was interpreted as mutation type if (1) ≥80% of tumor cells showed strong nuclear staining; (2) there was complete absence of nuclear staining in tumor cells with a positive internal control in the form of staining of a proportion of stromal and lymphoid cells; or (3) tumor cells showed definite cytoplasmic expression with variable nuclear staining [21, 22]. p53 staining was interpreted as wild type if expression patterns did not fulfill the aforementioned criteria [21, 22]. These thresholds for assigning abnormal p53 expression patterns were derived from published studies using p53 immunohistochemistry in high-grade serous carcinoma for which correlation between p53 expression and *TP53* mutation status has been well documented.

Next-generation targeted RNA sequencing

Histologic examination of hematoxylin and eosin-stained slides derived from formalin-fixed paraffin-embedded tissue (FFPE) was conducted by a pathologist and assessed for the presence of tumor. Ten cases were subjected to the MSK Solid Fusion ($n = 3$) and Archer Sarcoma FusionPlex ($n = 1$) Assays that utilize the Archer Anchored Multiplex PCR (AMP) technology as well as the TruSight RNA Fusion Panel ($n = 6$) (Illumina, San Diego, CA) to detect gene fusions and novel isoforms in solid tumors as previously described [19, 23]. RNA was extracted from macrodissected formalin-fixed, paraffin-embedded tumor tissue followed by cDNA synthesis and library preparation. Final targeted amplicons were sequenced on an Illumina MiSeq. Data were analyzed using Archer Software (version 4.0.10) or the STAR and BOWTIE2 aligners and Manta and JAFFA fusion callers, respectively [24–26].

Fluorescence in situ hybridization

In eight cases, fluorescence in situ hybridization (FISH) was performed on 4 µm FFPE tissue sections mounted on charged glass slides with regions of interest circled by one of the authors (SC). Custom probes using bacterial artificial chromosomes (BAC) covering and flanking *BCOR* (RP11-21D3, RP11-1105N2, RP11-37K20, and RP11-973F20), *JAZF1* (RP11-597H8, RP11-78F4, RP11-466B23, and RP11-945M23), *SUZ12* (RP11-55J8, RP11-299H3, RP11-398A1, and RP11-112D12) and *YWHAE* (RP11-105D11, RP11-1142D6, RP11-170J13, and RP11-806J5) genes were chosen according to the UCSC genome browser (http://genome.ucsc.edu) [19, 27]. BAC clones were retrieved from BACPAC sources of the Children's Hospital of Oakland Research Institute (Oakland, CA) (http://bacpac.chori.org). DNA from individual BACs were isolated according to the manufacturer's recommendations, labeled with different fluorochromes in a nick translation reaction, denatured, and hybridized to pretreated slides. Slides were incubated, washed, and mounted with DAPI in an antifade solution. The genomic location of each BAC set was confirmed by hybridizing them to normal metaphase chromosomes. Using a Zeiss fluorescence microscope (Zeiss Axioplan, Oberkochen, Germany), 200 successive nuclei were examined, controlled by Isis 5 software (Metasystems). A positive result was assigned when at least 20% of tumor nuclei displayed a break-apart signal corresponding to the likelihood of a fusion event. Nuclei with incomplete sets of signals were omitted from interpretation.

Results

High-grade transformation of LGESS may be associated with worse outcomes

The median patient age at the time of morphologic evidence of high-grade transformation was 54 (range, 45–74) years. Primary tumor sites were the uterine corpus ($n = 11$) and vagina ($n = 1$) (Table 1). Tumor stage was available in the 11 patients who presented with FIGO stages I ($n = 4$), II ($n = 4$), III ($n = 1$), and IV disease ($n = 2$). High-grade

Table 1 Clinical features.

Case	Age, years	Primary site	Stage[a]	Treatment prior to transformation	Time to transformation	Overall survival from transformation
1	53	Uterus	IIB	Surgery, hormonal therapy, chemotherapy	4 years	DOD, 2 years
2	55	Uterus	IIB	Surgery	0	NED, 2 years
3	53	Uterus	IVB	Surgery	0	DOD, 8 months
4	61	Vagina	I	Surgery	0	AWD, 12 months
5	45	Uterus	NA	Surgery	0	AWD, 2 years
6	51	Uterus	IIIA	Surgery	0	AWD, 20 months
7	74	Uterus	IB	Surgery	0	DOD, 2 years
8	50	Uterus	IIA	Surgery	10 years	AWD, 12 months
9	57	Uterus	IB	Surgery	11 years	NED, 8 years
10	69	Uterus	IVB	Surgery	0	DOD, 14 months
11	49	Uterus	IIA	Surgery	7 years	DOD, 18 months
12	71	Uterus	IB	Surgery	0	NED, 6 years

AWD alive with disease, *DOD* died of disease, *NA* not available, *NED* no evidence of disease.

[a]FIGO staging for uterine sarcomas was used for cases 1–3, 6–12; FIGO staging for vaginal cancer was used for case 4.

transformation was detected at the time of primary resection in eight patients and at the time of recurrence in four patients, 4–11 years after initial diagnosis. Only one patient received hormonal therapy and chemotherapy prior to detection of histologic high-grade transformation. The median overall survival was 22 months (range, 8 months to 8 years). Five patients died of disease 8 months to 2 years after transformation, four were alive with disease 12 months to 2 years after transformation, and three had no evidence of disease 2, 6, and 8 years after transformation.

Tumor cytologic atypia and mitotic activity and stromal sclerosis are observed in primary, synchronous metastatic, and metachronous high-grade transformation

Foci of histologically distinctive high-grade tumor in the background of an otherwise typical LGESS were seen in all primary ($n = 7$) and synchronous metastatic ($n = 2$) tumors. High-grade morphology without a low-grade component was seen in metachronous metastatic ($n = 3$) tumors only (Table 2). On low magnification, the high-grade component formed nodules that were sharply demarcated and readily distinguishable from areas of typical LGESS in ten tumors. The high-grade foci occupied 10–90% of the overall tumor and exhibited increased cytologic atypia and characteristically sclerotic and occasionally myxoid stroma (Fig. 1). When stromal sclerosis was present, it was often abundant and easily recognizable on low magnification in eight tumors. Myxoid matrix was evident in two. In contrast, the transition between high-grade and low-grade morphology was gradual in two tumors (Fig. 2). In all tumors, the high-grade component was composed of rounded epithelioid cells whose nuclei were one to two times larger than a lymphocyte and had vesicular chromatin and small to prominent nucleoli. The cytoplasm was scant to abundant and eosinophilic or amphophilic (Fig. 3). Slight spindling of the cells was frequently observed. Nuclear atypia of the high-grade foci was uniform/monomorphic in 11 tumors and variable/pleomorphic with scattered large multinucleated cells in one case (case 3). The median mitotic index in the high-grade foci was 16 (range, 6–30) per 10 high power fields (HPF) with atypical forms seen in one tumor (case 3). Delicate vasculature was present in the high-grade foci of all tumors, appearing compressed and lacking perivascular tumor cell whorls. Tumor necrosis was present in two cases.

Low-grade morphology was the predominant pattern in all primary tumors except for four where the high-grade component predominated (cases 7–9, 11). Conventional LGESS morphology was observed in the primary tumor in all cases, and in the synchronous metastatic tumor in two cases, characterized by sheets of bland fusiform to spindle cells with ovoid to slightly spindled nuclei, homogeneous chromatin, and scant cytoplasm associated with delicate vasculature and perivascular whorls reminiscent of proliferative phase endometrial stroma (Fig. 3). Variant features were also seen in five cases. Four tumors showed fibroblastic change accompanied by smooth muscle differentiation in three and myxoid matrix in two. One tumor demonstrated sex cord-like differentiation. The mitotic index was <1 per 10 HPF in the low-grade component of all tumors.

Transformed tumors may show loss of CD10, ER, and PR or diffuse cyclin D1 and BCOR staining with wild type p53 expression

CD10 staining was absent in the high-grade component of 5 of 11 tumors tested. ER and/or PR staining was also absent in the high-grade component of these five tumors (Table 2). The high-grade component of one tumor (case 2) showed CD10 and ER expression (95% of tumor cells), but markedly reduced PR expression (5%) (Fig. 4). The extent and intensity of CD10, ER, and PR staining were similar between high-grade and low-grade components in the other tumors. BCOR and cyclin D1 were positive in one tumor (case 6) and negative in the remaining eight tumors tested (Fig. 4). p53 staining patterns were wild type in the high-grade component of all eight tumors tested; p53 staining was also wild type in the low-grade component of five of the tumors.

Transformed tumors harbor LGESS associated gene fusions

FISH detected *JAZF1* rearrangements in seven (cases 2, 4, 5, 9–12) of eight tumors and confirmed *SUZ12* (cases 2 and 4) and *PHF1* (case 5) fusion partners in three. *JAZF1*, *PHF1*, *YWHAE*, and *BCOR* rearrangements were not detected in one tumor (case 6) (Table 2).

Targeted RNA sequencing was employed in nine tumors with sufficient material (cases 1, 3, 6–12), including four with *JAZF1* rearrangement (cases 9–12) and no known fusion partner as well as one tumor lacking *JAZF1*, *PHF1*, *YWHAE*, and *BCOR* rearrangement (case 6) by FISH. Fusions were detected in eight tumors (Table 2), including *JAZF1-SUZ12* ($n = 4$), *JAZF1-PHF1* ($n = 2$), *EPC1-PHF1* ($n = 1$), and *BRD8-PHF1* ($n = 1$). No fusions were detected by the MSK Solid Fusion Assay and TruSight RNA Fusion Panel in case 3. None of the nine tumors analyzed by sequencing showed *YWHAE* or *BCOR* genetic alterations.

Absent or significantly decreased CD10, ER, and/or PR expression was observed in tumors with *JAZF1-SUZ12* ($n = 2$), *JAZF1-PHF1* ($n = 3$), and *BRD8-PHF1* ($n = 1$) fusion (Table 2).

Table 2 Histologic, immunophenotypic and molecular genetic features.

		Histology		Mitotic index		Immunoprofile of HG component						
Case	HG site	HG	LG	HG	LG	CD10	ER	PR	BCOR	Cyclin D1	p53	Fusion
1	S	Round cells with vesicular chromatin, prominent nucleoli, sclerotic stroma	Conventional, sex cord-like differentiation	8	<1	+	+, 95%	+, 95%	−	−	WT	*EPC1-PHF1*
2	P	Large cells with vesicular chromatin, small nucleoli, sclerotic and myxoid stroma	Conventional, fibroblastic differentiation and myxoid change	30	<1	+	+, 95%	+, 5%	−	−	WT	*JAZF1-SUZ12*
3	P	Large epithelioid cells with prominent nucleoli, multinucleation, sclerotic stroma	Conventional, fibroblastic and smooth muscle differentiation	16	<1	+	NP	NP	NP	NP	NP	ND
4	P	Round cells with vesicular chromatin, small nucleoli, necrosis	Conventional, fibroblastic and smooth muscle differentiation, myxoid change	10	<1	NP	NP	NP	−	NP	NP	*JAZF1-SUZ12*
5	P	Round cells with vesicular chromatin, small nucleoli, sclerotic and myxoid stroma	Conventional, fibroblastic and smooth muscle differentiation	18	<1	−	−	−	−	−	NP	*JAZF1-PHF1*
6	S	Large spindled and epithelioid cells with prominent nucleoli	Conventional	9	<1	+	+, 95%	+, 95%	+	+	NP	*JAZF1-SUZ12*
7	P	Round cells with vesicular chromatin, small nucleoli,	Conventional	16	<1	+	+, 95%	+, 95%	−	−	WT	*JAZF1-SUZ12*
8	M	Large epithelioid cells with vesicular chromatin, small nucleoli, sclerotic stroma	Conventional (P only)	30	<1	−	−	−	NP	−	WT	*BRD8-PHF1*
9	M	Large epithelioid cells with vesicular chromatin, small nucleoli, sclerotic stroma	Conventional (P only)	20	<1	−	−	−	NP	−	WT	*JAZF1-PHF1*
10	P	Large epithelioid cells with vesicular chromatin, small nucleoli, sclerotic stroma	Conventional	30	<1	−	−	−	NP	NP	WT	*JAZF1-SUZ12*
11	M	Round cells with vesicular chromatin, small nucleoli	Conventional (P only)	10	<1	−	−	NP	NP	NP	WT	*JAZF1-PHF1*
12	P	Epithelioid cells with open chromatin, small nucleoli, sclerotic stroma	Conventional	6	<1	+	+, 95%	+, 95%	NP	−	WT	*JAZF1-SUZ12*

HG high grade, *LG* low grade, *M* metachronous, *NP* not performed, *P* primary; *S* synchronous, *WT* wild type.

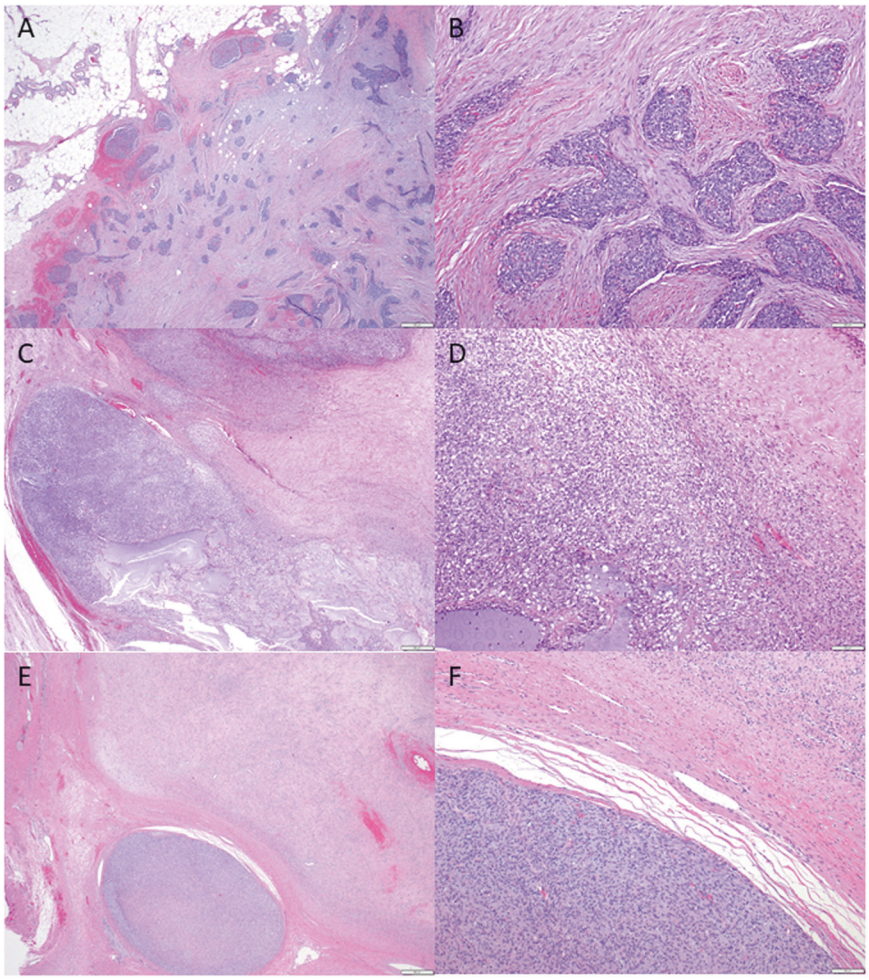

Fig. 1 High-grade components forming nodules. **a** Desmoplastic stroma surround **b** variably shaped nodules of round cells. **c** Sclerotic stroma surrounds a nodule of **d** round cells associated with myxoid matrix. **e, f** A circumscribed nodule of high-grade round cells (bottom and left) is separated from the low-grade component (top and right) by a dense fibrous band.

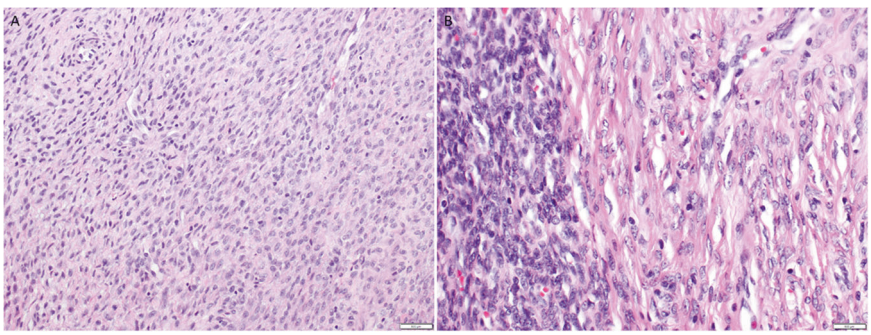

Fig. 2 Gradual transition between low- and high-grade components of endometrial stromal sarcoma. a A low-grade component composed of cells with small hyperchromatic nuclei and scant eosinophilic cytoplasm (left) merges with a high-grade component composed of cells with slightly larger nuclei, open chromatin, prominent nucleoli, and increased amphophilic cytoplasm (right). **b** Dense proliferation of small spindle cells typical of LGESS (left) to a high-grade component with increased cytologic atypia (right).

Discussion

In this study, we show that high-grade morphologic transformation may occur in LGESS that lack *YWHAE* and *BCOR* genetic abnormalities. High-grade transformation may be seen in primary, metastatic, or recurrent tumor and is characterized by histologically distinctive nodular foci of round cells with nuclear enlargement, prominent nucleoli, and brisk mitotic activity that contrast with LGESS morphology. This is often associated with variably prominent sclerotic or myxoid stroma. Foci of high-grade transformation often comprise

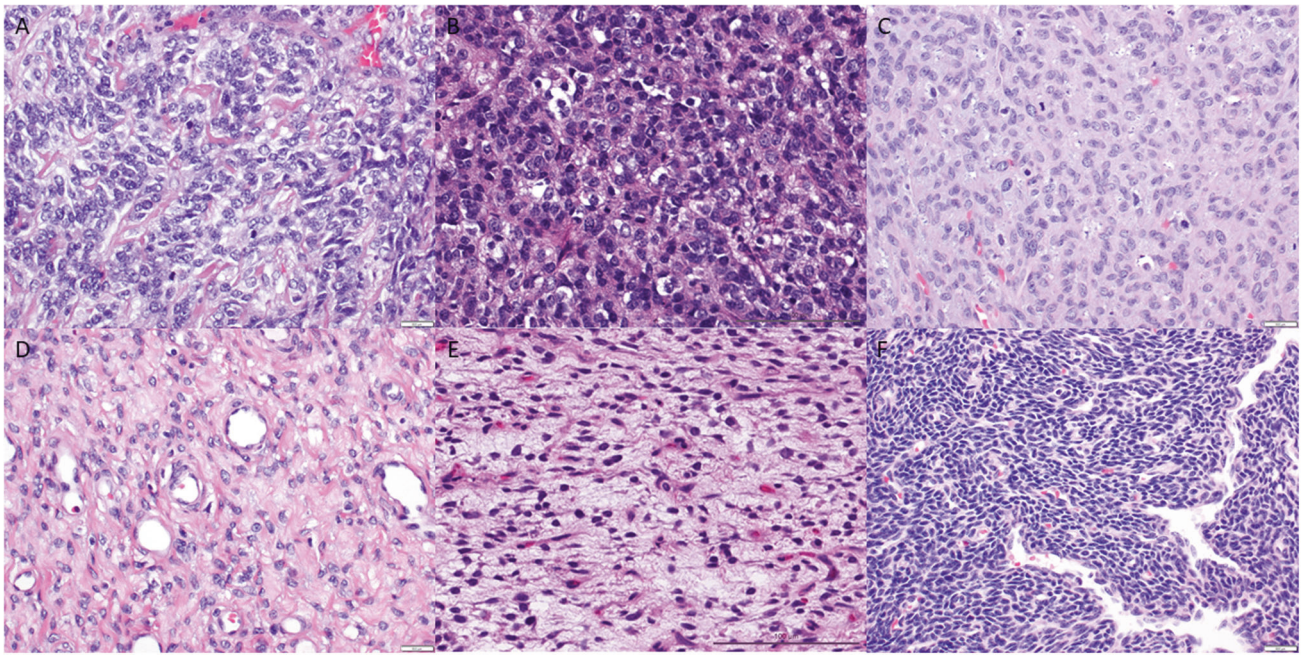

Fig. 3 Paired foci of high- and low-grade components. High-grade components are composed of enlarged epithelioid cells with round nuclei, heterogeneous chromatin, and moderate amounts of amphophilic or eosinophilic cytoplasm associated with brisk mitotic activity and forming (**a**) trabeculae or (**b**), (**c**) sheets. Low-grade components show variant **d** fibrous, **e** myxoid, and **f** conventional histology.

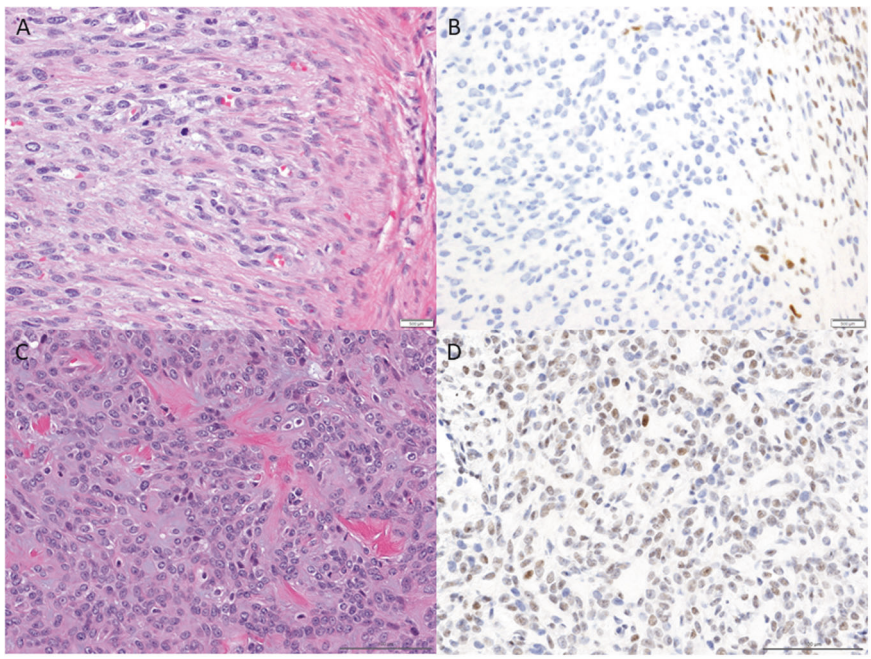

Fig. 4 Distinct PR and BCOR expression profiles of high-grade components. a The high-grade component demonstrates **b** loss of PR expression with myometrium (right) serving as an internal positive control. **c** The high-grade component shows **d** diffuse and strong nuclear BCOR staining which is often associated with HGESS.

uniform round cells that demonstrate diminished or absent CD10, ER, and PR expression and occasionally BCOR and cyclin D1 expression. *TP53* mutations are unlikely to be involved in the development of high-grade transformation based on wild-type (normal) p53 expression. Most of these lesions harbor rearrangements involving *JAZF1* or *PHF1* genes, molecular events that are common in LGESS.

All tumors demonstrated a low-grade component with conventional and/or variant LGESS features, including sex cord-like and smooth muscle differentiation as well as fibroblastic or fibromyxoid change. The mitotic index in

these foci was <1 per 10 HPF, similar to most LGESS. In contrast, the high-grade foci in all tumors exhibited nuclear atypia and brisk mitotic activity frequently with an index of at least 10 per 10 HPF. In all tumors, these high-grade regions were cytologically distinct from the low-grade component and were recognizable on low magnification in most cases. *JAZF1* and *PHF1* rearrangements which are frequently present in LGESS with conventional and/or variant histologic features, underpin 10 of 11 tumors. Currently, the designation HGESS is confined to tumors exhibiting *YWHAE* or *BCOR* genetic abnormalities, which may be associated with a low-grade spindle cell component resembling fibrous or fibromyxoid LGESS. None of the studies reporting bona fide HGESS harboring *YWHAE* or *BCOR* genetic abnormalities demonstrate conventional LGESS histology. As a group, the tumors we report are histogenetically distinct from the usual *YWHAE* or *BCOR* associated HGESS and this represents a third category of neoplasms where the term HGESS is appropriate.

While the clinical data are limited, there are two features of transformed endometrial stromal sarcomas that are clinically relevant. Our findings suggest a trend toward aggressive behavior among tumors with high-grade transformation compared with published outcomes of LGESS. Approximately 40% (5 of 12) of our patients died of disease 8–18 months after transformation. Eight patients (67%) had histologic evidence of transformation at the time of initial diagnosis. However, 33% (4 of 12) of patients were found to have histologic evidence of transformation at a time period distant from the initial diagnosis, suggesting that the disease may escape hormone blockade and progress years later.

Based on our study and the very few prior reports published in the literature, high-grade transformation of LGESS is exceedingly rare. Among eight published cases for which the morphologic and immunohistochemical features are adequately detailed, three may represent *YWHAE-NUTM2* HGESS based on our review of the reported histologic and immunophenotypic features [13, 15, 28]. Two studies with genotyping analysis identified *JAZF1-SUZ12* fusions in lesions classified as HGESS or undifferentiated uterine sarcoma [16, 29], and one of these appears to represent a bona fide LGESS with high-grade transformation based on the provided figures [16]. Two tumors in another study demonstrated LGESS morphology with an abrupt transition to a high-grade component and did not harbor *JAZF1*, *PHF1*, *YWHAE*, and *CCND1* rearrangements by FISH [6]. *EPC1-SUZ12*, *EPC1-BCOR*, *BRD8-PHF1*, and *JAZF1-BCORL1* fusions were also recently reported in endometrial stromal sarcomas with low- and high-grade components [19, 23, 30, 31]. It is unclear whether tumors from either study represent LGESS with high-grade transformation or bona fide HGESS that may demonstrate low-grade foci similar to lesions harboring *YWHAE-NUTM2* fusion and *BCOR* internal tandem duplication.

This study has several limitations. As with most other studies of rare cancers including those describing HGESS with *YWHAE* or *BCOR* genetic abnormalities, clinical data are limited. However, the presence of high-grade transformation appears associated with an accelerated disease course when compared with typical LGESS. We were also unable to identify fusions by targeted RNA sequencing in one tumor. While common rearrangements involving genes such as *SUZ12*, *JAZF1*, *PHF1*, *YWHAE*, and *BCOR* were not found using this method, this tumor likely harbors an alternative fusion that may be identifiable by whole transcriptome sequencing.

In conclusion, histologic high-grade transformation may rarely occur in LGESS and is characterized by nuclear atypia and mitotic activity that surpasses features acceptable for LGESS. These tumors often harbor gene fusions that are typically associated with LGESS. The clinical significance of this unusual morphologic finding remains uncertain, and long-term multi-institutional studies are required.

Compliance with ethical standards

Conflict of interest The authors have no conflicts of interest to disclose.

Publisher's note Springer Nature remains neutral with regard to jurisdictional claims in published maps and institutional affiliations.

References

1. Norris HJ, Taylor HB. Mesenchymal tumors of the uterus. I. A clinical and pathological study of 53 endometrial stromal tumors. Cancer. 1966;19:755–66.
2. Chang KL, Crabtree GS, Lim-Tan SK, Kempson RL, Hendrickson MR. Primary uterine endometrial stromal neoplasms. A clinicopathologic study of 117 cases. Am J Surg Pathol. 1990; 14:415–38.
3. Croce S, Hostein I, Ribeiro A, Garbay D, Velasco V, Stoeckle E, et al. YWHAE rearrangement identified by FISH and RT-PCR in endometrial stromal sarcomas: genetic and pathological correlations. Mod Pathol. 2013;26:1390–400.
4. Lee CH, Marino-Enriquez A, Ou W, Zhu M, Ali RH, Chiang S, et al. The clinicopathologic features of YWHAE-FAM22 endometrial stromal sarcomas: a histologically high-grade and clinically aggressive tumor. Am J Surg Pathol. 2012;36:641–53.
5. Lee CH, Ou WB, Marino-Enriquez A, Zhu M, Mayeda M, Wang Y, et al. 14-3-3 fusion oncogenes in high-grade endometrial stromal sarcoma. Proc Natl Acad Sci USA. 2012;109:929–34.
6. Sciallis AP, Bedroske PP, Schoolmeester JK, Sukov WR, Keeney GL, Hodge JC, et al. High-grade endometrial stromal sarcomas: a clinicopathologic study of a group of tumors with heterogenous morphologic and genetic features. Am J Surg Pathol. 2014; 38:1161–72.
7. Lewis N, Soslow RA, Delair DF, Park KJ, Murali R, Hollmann TJ, et al. ZC3H7B-BCOR high-grade endometrial stromal sarcomas: a

report of 17 cases of a newly defined entity. Mod Pathol. 2018; 31:674–84.
8. Hoang LN, Aneja A, Conlon N, Delair DF, Middha S, Benayed R, et al. Novel high-grade endometrial stromal sarcoma: a morphologic mimicker of myxoid leiomyosarcoma. Am J Surg Pathol. 2017;41:12–24.
9. Chiang S, Lee CH, Stewart CJR, Oliva E, Hoang LN, Ali RH, et al. BCOR is a robust diagnostic immunohistochemical marker of genetically diverse high-grade endometrial stromal sarcoma, including tumors exhibiting variant morphology. Mod Pathol. 2017;30:1251–61.
10. Juckett LT, Lin DI, Madison R, Ross JS, Schrock AB, Ali S. A pan-cancer landscape analysis reveals a subset of endometrial stromal and pediatric tumors defined by internal tandem duplications of BCOR. Oncology. 2019;96:101–9.
11. Marino-Enriquez A, Lauria A, Przybyl J, Ng TL, Kowalewska M, Debiec-Rychter M, et al. BCOR internal tandem duplication in high-grade uterine sarcomas. Am J Surg Pathol. 2018;42:335–41.
12. Lee CH, Ali RH, Rouzbahman M, Marino-Enriquez A, Zhu M, Guo X, et al. Cyclin D1 as a diagnostic immunomarker for endometrial stromal sarcoma with YWHAE-FAM22 rearrangement. Am J Surg Pathol. 2012;36:1562–70.
13. Ohta Y, Suzuki T, Omatsu M, Hamatani S, Shiokawa A, Kushima M, et al. Transition from low-grade endometrial stromal sarcoma to high-grade endometrial stromal sarcoma. Int J Gynecol Pathol. 2010;29:374–7.
14. Amant F, Woestenborghs H, Vandenbroucke V, Berteloot P, Neven P, Moerman P, et al. Transition of endometrial stromal sarcoma into high-grade sarcoma. Gynecol Oncol. 2006;103:1137–40.
15. Cheung AN, Ng WF, Chung LP, Khoo US. Mixed low grade and high grade endometrial stromal sarcoma of uterus: differences on immunohistochemistry and chromosome in situ hybridisation. J Clin Pathol. 1996;49:604–7.
16. Kurihara S, Oda Y, Ohishi Y, Iwasa A, Takahira T, Kaneki E, et al. Endometrial stromal sarcomas and related high-grade sarcomas: immunohistochemical and molecular genetic study of 31 cases. Am J Surg Pathol. 2008;32:1228–38.
17. Smith ML, Faaborg LL, Newland JR. Dedifferentiation of endolymphatic stromal myosis to poorly differentiated uterine stromal sarcoma. Gynecol Oncol. 1980;9:108–13.
18. Garg K, Leitao MM Jr., Wynveen CA, Sica GL, Shia J, Shi W, et al. p53 overexpression in morphologically ambiguous endometrial carcinomas correlates with adverse clinical outcomes. Mod Pathol. 2010;23:80–92.
19. Cotzia P, Benayed R, Mullaney K, Oliva E, Felix A, Ferreira J, et al. Undifferentiated uterine sarcomas represent under-recognized high-grade endometrial stromal sarcomas. Am J Surg Pathol. 2019; 43:662–9.
20. Calhoun BC, Collins LC. Predictive markers in breast cancer: an update on ER and HER2 testing and reporting. Semin Diagn Pathol. 2015;32:362–9.
21. Kobel M, Ronnett BM, Singh N, Soslow RA, Gilks CB, McCluggage WG. Interpretation of p53 immunohistochemistry in endometrial carcinomas: toward increased reproducibility. Int J Gynecol Pathol. 2019;38:S123–S31.
22. Yemelyanova A, Vang R, Kshirsagar M, Lu D, Marks MA, Shih Ie M, et al. Immunohistochemical staining patterns of p53 can serve as a surrogate marker for TP53 mutations in ovarian carcinoma: an immunohistochemical and nucleotide sequencing analysis. Mod Pathol. 2011;24:1248–53.
23. Dickson BC, Lum A, Swanson D, Bernardini MQ, Colgan TJ, Shaw PA, et al. Novel EPC1 gene fusions in endometrial stromal sarcoma. Genes Chromosomes Cancer. 2018;57:598–603.
24. Chen X, Schulz-Trieglaff O, Shaw R, Barnes B, Schlesinger F, Kallberg M, et al. Manta: rapid detection of structural variants and indels for germline and cancer sequencing applications. Bioinformatics. 2016;32:1220–2.
25. Liu S, Tsai WH, Ding Y, Chen R, Fang Z, Huo Z, et al. Comprehensive evaluation of fusion transcript detection algorithms and a meta-caller to combine top performing methods in paired-end RNA-seq data. Nucleic Acids Res. 2016; 44:e47.
26. Zheng Z, Liebers M, Zhelyazkova B, Cao Y, Panditi D, Lynch KD, et al. Anchored multiplex PCR for targeted next-generation sequencing. Nat Med. 2014;20:1479–84.
27. Chiang S, Ali R, Melnyk N, McAlpine JN, Huntsman DG, Gilks CB, et al. Frequency of known gene rearrangements in endometrial stromal tumors. Am J Surg Pathol. 2011;35:1364–72.
28. Roy M, Kumar S, Bhatla N, Ray MD, Kumar L, Jain D, et al. Androgen receptor expression in endometrial stromal sarcoma: correlation with clinicopathologic features. Int J Gynecol Pathol. 2017;36:420–7.
29. Koontz JI, Soreng AL, Nucci M, Kuo FC, Pauwels P, van Den Berghe H, et al. Frequent fusion of the JAZF1 and JJAZ1 genes in endometrial stromal tumors. Proc Natl Acad Sci USA. 2001;98: 6348–53.
30. Allen AJ, Ali SM, Gowen K, Elvin JA, Pejovic T. A recurrent endometrial stromal sarcoma harbors the novel fusion JAZF1-BCORL1. Gynecol Oncol Rep. 2017;20:51–3.
31. Micci F, Brunetti M, Dal Cin P, Nucci MR, Gorunova L, Heim S, et al. Fusion of the genes BRD8 and PHF1 in endometrial stromal sarcoma. Genes Chromosomes Cancer. 2017;56:841–5.

Affiliations

Youran Zou[1] · Gulisa Turashvili[2,3] · Robert A. Soslow[4] · Kay J. Park[4] · Sabrina Croce[5] · W. Glenn McCluggage[6] · Colin J. R. Stewart[7,8] · Yoshinao Oda[9] · Esther Oliva[10,11] · Robert H. Young[10,11] · Arnaud Da Cruz Paula[12] · Kimberly Dessources[12] · Charles W. Ashley[12] · Martee L. Hensley[13] · Stephen Yip[14,15,16] · Britta Weigelt[4] · Ryma Benayed[4] · Cristina R. Antonescu[4] · Cheng-Han Lee[15,16] · Sarah Chiang[4]

[1] Department of Pathology, Oakland Medical Center, Kaiser Permanente, Oakland, CA, USA

[2] Department of Pathology and Laboratory Medicine, Mount Sinai Hospital, Toronto, ON, Canada

[3] Department of Pathology and Laboratory Medicine, University of Toronto, Toronto, ON, Canada

[4] Department of Pathology, Memorial Sloan Kettering Cancer Center, New York, NY, USA

[5] Department of Biopathology, Institut Bergonié, Comprehensive Cancer Center, Bordeaux, France

[6] Department of Pathology, Belfast Health and Social Care Trust, Belfast, Northern Ireland, UK

[7] Department of Pathology, King Edward Memorial Hospital, Perth, WA, Australia

[8] School of Women's and Infants' Health, University of Western Australia, Perth, WA, Australia

[9] Department of Anatomic Pathology, Graduate School of Medical Sciences, Kyushu University, Higashi-ku, Fukuoka, Japan

[10] Department of Pathology, Massachusetts General Hospital, Boston, MA, USA

[11] Department of Pathology, Harvard Medical School, Boston, MA, USA

[12] Department of Surgery, Gynecologic Oncology Service, Memorial Sloan Kettering Cancer Center, New York, NY, USA

[13] Department of Medicine, Gynecologic Medical Oncology Service, Memorial Sloan Kettering Cancer Center, New York, NY, USA

[14] Department of Pathology and Laboratory Medicine, Vancouver General Hospital, Vancouver, BC, Canada

[15] Department of Pathology and Laboratory Medicine, BC Cancer, Vancouver, BC, Canada

[16] Department of Pathology and Laboratory Medicine, University of British Columbia, Vancouver, BC, Canada